Testing Λ-free $f(Q)$ cosmology

José Ferreira,[1,2,*] Tiago Barreiro,[1,3,†] José P. Mimoso,[1,2,‡] and Nelson J. Nunes[1,2,§]

[1]*Instituto de Astrofísica e Ciências do Espaço, Faculdade de Ciências da Universidade de Lisboa, Campo Grande, Edificio C8, P-1749-016, Lisboa, Portugal*

[2]*Departamento de Física, Faculdade de Ciências da Universidade de Lisboa, Campo Grande, Edificio C8, P-1749-016, Lisboa, Portugal*

[3]*ECEO, Universidade Lusófona de Humanidades e Tecnologias, Campo Grande, 376, 1749-024 Lisboa, Portugal*

(Received 26 June 2023; accepted 31 August 2023; published 22 September 2023)

We study a model of symmetric teleparallel gravity that is able to account for the current accelerated expansion of the Universe without the need for a dark energy component. We investigate this model by making use of dynamical system analysis techniques to identify the regions of the parameter space with viable cosmologies and constrain it using type-Ia supernovae (SnIa) and cosmic microwave background (CMB) data, and make forecasts using standard siren (SS) events. We conclude that this model is disfavored with respect to ΛCDM, and forthcoming standard siren events can be decisive in testing the viability of the model.

DOI: 10.1103/PhysRevD.108.063521

I. INTRODUCTION

The standard model of cosmology, referred to as ΛCDM, provides us with the most accurate description of the Universe at large scales. However, despite its successes, it is not devoid of difficulties [1]. One of the most debated of its shortcomings is the origin of the cosmological constant, introduced to explain the current accelerated expansion of the Universe. Also, tensions in the value of the expansion rate obtained from low-redshift against high-redshift data motivate the search for alternative descriptions.

Recently, it has been shown that two gravitational theories equivalent to general relativity (GR) exist, one based solely on nonmetricity and the other based solely on torsion. This equivalence is referred to as the geometrical trinity of gravity [2]. Generalizations of these formulations have been considered as $f(T)$, the teleparallel gravity, or $f(Q)$, the symmetric teleparallel gravity [3–5]. These theories are particularly interesting, as even if they only produce slight deviations from ΛCDM at the background level [6], they may give rise to signatures in the evolution of the density perturbations [7] and in the propagation of gravitational waves [8], potentially being able to solve the challenges that ΛCDM faces [9–16].

With the development of new techniques in gravitational wave (GW) astronomy, cosmologists will soon have access to a new and exciting source of data: standard siren (SS) events, characterized by the direct measurement of both the luminosity distance and the redshift of merging compact objects. Unfortunately, up to the current date, only GW170817 [17] has been confirmed as a SS event; a suggested electromagnetic (EM) counterpart to GW190521 [18] was proposed in [19].

In this work, we focus on a model of $f(Q)$ gravity able to account for the late-time accelerated expansion of the Universe without adding a cosmological constant. We develop a dynamical system analysis in order to look for regions in parameter space that yield viable cosmologies, and we constrain this model by making use of both high- and low-redshift observables—namely, type-Ia supernovae (SnIa) and the cosmic microwave background (CMB)—and in addition, we make forecasts using mock catalogs of SS events made for the Laser Interferometer Space Antenna (LISA) [20,21] and the Einstein Telescope (ET). An online repository complementary to this analysis is publicly available at [22].

This work is organized as follows: In Sec. II, we provide a brief introduction to the formalism behind $f(Q)$ cosmology and introduce the specific model we will be working with. In Sec. III, we perform a dynamical system analysis applied to the model to identify the regions of the phase space leading to late-time acceleration. In Sec. IV, we introduce the datasets we use. In Sec. V, we show the constraints given by the datasets introduced before. Finally, in Sec. VI, we make an overview of this work.

II. COSMOLOGY IN $f(Q)$

In this work, we consider a theory of modified gravity based on an arbitrary function of the nonmetricity scalar. The action for such a theory of gravity reads

*jpmferreira@ciencias.ulisboa.pt
†tmbarreiro@ulusofona.pt
‡jpmimoso@ciencias.ulisboa.pt
§njnunes@ciencias.ulisboa.pt

$$S = \int \sqrt{-g}\left[-\frac{c^4}{16\pi G} f(Q) + \mathcal{L}_m\right] d^4x, \tag{1}$$

where Q is the nonmetricity scalar that is defined as [23]

$$Q = -\frac{1}{4} Q_{\alpha\beta\gamma} Q^{\alpha\beta\gamma} + \frac{1}{2} Q_{\alpha\beta\gamma} Q^{\gamma\beta\alpha} + \frac{1}{4} Q_\alpha Q^\alpha - \frac{1}{2} Q_\alpha \tilde{Q}^\alpha, \tag{2}$$

with $Q_{\alpha\mu\nu} = \nabla_\alpha g_{\mu\nu}$, and the two independent contractions of the nonmetricity tensor are

$$Q_\mu = Q_\mu{}^\alpha{}_\alpha, \qquad \tilde{Q}^\mu = Q_\alpha{}^{\alpha\mu}. \tag{3}$$

When varying the action in Eq. (1) with respect to the metric, one obtains the field equations [24]

$$\frac{2}{\sqrt{-g}} \nabla_\alpha (\sqrt{-g} f_Q P^{\alpha\mu}{}_\nu) + \frac{1}{2} \delta^\mu_\nu f + f_Q P^{\mu\alpha\beta} Q_{\nu\alpha\beta} = \frac{8\pi G}{c^4} T^\mu{}_\nu, \tag{4}$$

where f_Q represents the partial derivative of $f(Q)$ with respect to Q. $P^{\alpha\mu\nu}$, referred to as the nonmetricity conjugate, is defined as

$$P^\alpha{}_{\mu\nu} = -\frac{1}{2} L^\alpha{}_{\mu\nu} + \frac{1}{4}(Q^\alpha - \tilde{Q}^\alpha) - \frac{1}{4} \delta^\alpha_{(\mu} Q_{\nu)}, \tag{5}$$

where $L^\alpha{}_{\mu\nu}$ is the disformation tensor

$$L^\lambda{}_{\mu\nu} = \frac{1}{2} g^{\lambda\beta}(-Q_{\mu\beta\nu} - Q_{\nu\beta\mu} + Q_{\beta\mu\nu}). \tag{6}$$

We use the coincident gauge to specify the affine connection [3,23,25] and restrict our analysis to a flat, homogeneous and isotropic universe, described by the FLRW metric

$$ds^2 = -c^2 dt^2 + a^2(t)(dx^2 + dy^2 + dz^2), \tag{7}$$

where $a(t)$ is the scale factor of the universe, and t is cosmic time t. Under these assumptions, the nonmetricity scalar defined in Eq. (2) simplifies to [24]

$$Q = 6H^2, \tag{8}$$

where $H = \dot{a}/a$ is the Hubble function. Considering a universe permeated by a perfect fluid composed of both matter and radiation, the modified first Friedmann equation reads [24]

$$6 f_Q H^2 - \frac{1}{2} f = 8\pi G(\rho_m + \rho_r). \tag{9}$$

As stated in [26], the covariant derivative of the stress-energy momentum tensor is still zero, meaning that each component of the fluid obeys the standard continuity equation

$$\dot{\rho} + 3\frac{\dot{a}}{a}\left(\rho + \frac{P}{c^2}\right) = 0, \tag{10}$$

where P stands for pressure. This means that the scaling for each component is the same as in ΛCDM, and we can rewrite Eq. (9) as

$$\frac{2Qf_Q - f}{Q_0} = \frac{\Omega_m}{a^3} + \frac{\Omega_r}{a^4}, \tag{11}$$

where $\Omega_i = 8\pi G\rho_{i,0}/3H_0^2$ and $E \equiv H/H_0$, with the index 0 denoting the value of that quantity today.

This modification of gravity also changes the equation of motion for the propagation of gravitational waves [24]:

$$\bar{h}_A'' + 2\mathcal{H}(1 + \delta(z))\bar{h}_A' + k^2 \bar{h}_A = 0, \tag{12}$$

where $A = \times, +$ represent the polarizations of the GWs. The previous equation differs from the case of ΛCDM by an additional friction factor, $\delta(z)$, that for an $f(Q)$ model takes the form

$$\delta(z) = \frac{d \ln f_Q}{2\mathcal{H} d\eta}. \tag{13}$$

Following [8], this leads to a modification to the luminosity distance for a GW event, such that

$$d_{\mathrm{GW}}(z) = \sqrt{\frac{f_Q^{(0)}}{f_Q}} d_L(z), \tag{14}$$

where $f_Q^{(0)}$ is the function f_Q computed at the present day and $d_L(z)$ is the standard luminosity distance function.

A. $f(Q)$ cosmological model

In this work, we consider a model that differs from the standard interpretation of gravity—i.e., GR, for which $f(Q) = Q$—by taking a multiplicative exponential term of the form [27]

$$f(Q) = Qe^{\lambda Q_0/Q}, \tag{15}$$

where λ is a constant; however, it is not a free parameter. As we will see in Sec. III, λ is related to the abundance of matter today and has to be positive for a viable universe.

By making use of Eq. (8), we can see that the extra multiplicative term in this model is an exponential that is inversely proportional to the Hubble function. Given that the Hubble function increases with redshift, this model exponentially approaches the case where $f(Q) = Q$, meaning that it has GR as a limit case at early times.

Inserting the specific form of $f(Q)$ into Eq. (11), we obtain the modified first Friedmann equation for this model, which reads

$$(E^2 - 2\lambda)e^{\lambda/E^2} = \Omega_m(1+z)^3 + \Omega_r(1+z)^4, \quad (16)$$

where $E(z) \equiv H(z)/H_0$.

As hinted before, this model falls back to GR in the limit of high redshifts. For $z \gg 1$, Eq. (16) is approximately equal to

$$E^2 \approx \Omega_m(1+z)^3 + \Omega_r(1+z)^4 + \lambda, \quad (17)$$

which corresponds to a ΛCDM universe with $\Omega_\Lambda = \lambda$, where its effect is negligible at these early times. When evaluated today ($E^2 \approx 1$), Eq. (16) reduces to

$$E^2 \approx e^{-\lambda}\Omega_m(1+z)^3 + e^{-\lambda}\Omega_r(1+z)^4 + 2\lambda, \quad (18)$$

which corresponds once again to a ΛCDM universe, but now with $\Omega_\Lambda = 2\lambda$ and a correction in the relative abundance of matter and radiation. We note that, in the absence of matter fields, $\rho_m = \rho_r = 0$, we obtain a de Sitter universe with $\lambda = 1/2$.

If we insert the form of the function $f(Q)$ into Eq. (14), then we obtain the luminosity distance function for this specific model, which now reads

$$d_{\mathrm{GW}}(z) = \sqrt{\frac{1-\lambda}{1-\lambda/E^2}}e^{\frac{\lambda}{2}(1-1/E^2)}d_L(z). \quad (19)$$

This model was originally proposed in [27], where it was shown to be statistically equivalent to ΛCDM for tests using low-redshift measurements. Additionally, it has been shown to pass big bang nucleosynthesis constraints [28].

III. DYNAMICAL SYSTEM ANALYSIS

In order to perform our dynamical systems analysis, we can start by rewriting Eq. (16) as

$$1 = \frac{e^{-\lambda/E^2}}{E^2}\left(\frac{\Omega_m}{a^3} + \frac{\Omega_r}{a^4}\right) + \frac{2\lambda}{E^2}. \quad (20)$$

Defining the quantities

$$x_1 \equiv \frac{\Omega_m}{E^2 e^{\lambda/E^2} a^3}, \quad x_2 \equiv \frac{\Omega_r}{E^2 e^{\lambda/E^2} a^4}, \quad x_3 \equiv \frac{2\lambda}{E^2}, \quad (21)$$

where x_1 is related to the evolution of the matter density in the universe, x_2 to the radiation density, and x_3 to the parameter λ, they satisfy

$$x_1 + x_2 + x_3 = 1. \quad (22)$$

This equation shows that one of our coordinates in phase space is fully determined by the value of the other two. As such, without loss of generality, we choose to work with x_1 and x_2 alone.

Differentiating both x_1 and x_2 with respect to the number of e-folds, $N = \ln a$, we obtain

$$x_1' = -x_1\left((1 + x_1 + x_2)\frac{E'}{E} + 3\right), \quad (23)$$

$$x_2' = -x_2\left((1 + x_1 + x_2)\frac{E'}{E} + 4\right), \quad (24)$$

where the prime denotes the derivative with respect to N, and the ratio E'/E can be expressed as a function of both x_1 and x_2 by

$$\frac{E'}{E} = \frac{-(3x_1 + 4x_2)}{2 - (x_1 + x_2) + (x_1 + x_2)^2}. \quad (25)$$

A. Fixed points

For this dynamical system, we find three distinct fixed points. Their locations and corresponding stability is presented in Table I.

Fixed point *I* corresponds to a λ-dominated regime and is the only stable fixed point in our system. It is located at x_1, $x_2 = 0$, corresponding to

$$E^2 = 2\lambda, \quad (26)$$

and therefore it only exists if λ is positive.

By integrating the previous equation, we obtain the evolution of the scale factor as a function of time:

$$a = e^{\sqrt{2\lambda}H_0 t}, \quad (27)$$

meaning that we have an exponential expansion, corresponding to a point of eternal inflation.

The fixed point *II* corresponds to a matter-dominated regime located at $x_1 = 1$ and $x_2 = 0$, implying that $\lambda = 0$. It is a saddle node with attracting trajectories along the direction of fixed point *III*. Setting $\lambda = 0$ in Eq. (15), we have $f(Q) = Q$, corresponding to the GR limit—more specifically, a cold dark matter (CDM) universe, since this model does not include a cosmological constant.

As for fixed point *III*, it corresponds to a radiation-dominated regime and is located at $x_1 = 0$ and $x_2 = 1$. It is an unstable node, and like fixed point *II*, it is located in a

TABLE I. Fixed points and corresponding stability for the dynamical system.

Point	Type	x_1	x_2	Stability	Eigenvalues
I	λ-dominated	0	0	Stable	$(-4, -3)$
II	Matter-dominated	1	0	Saddle	$(3, -1)$
III	Radiation-dominated	0	1	Unstable	(4, 1)

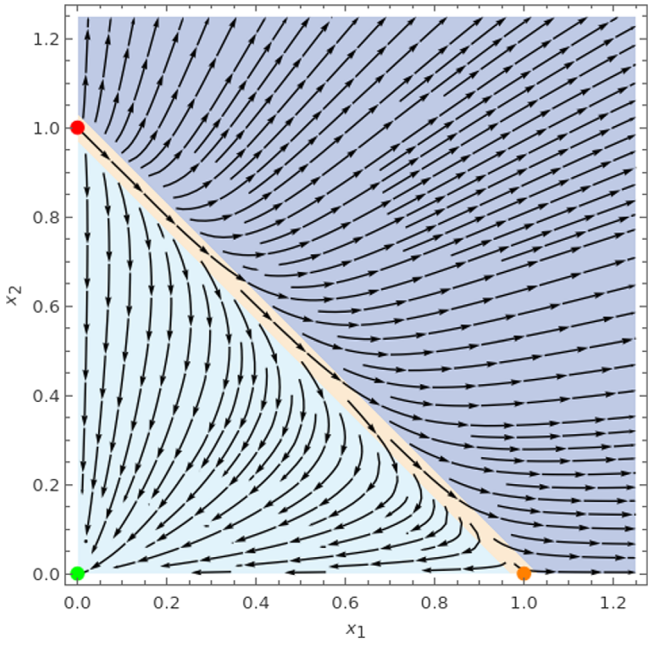

FIG. 1. Stream plot of the phase space for the dynamical system where fixed point *I* (stable) is represented in green, fixed point *II* (saddle) is in orange, and fixed point *III* (unstable) is in red. The light blue marks the region where $\lambda > 0$, the light brown region corresponds to $\lambda = 0$, and the dark blue region corresponds to $\lambda < 0$.

region where $\lambda = 0$, meaning that it is in the GR limit with $f(Q) = Q$.

B. Trajectories

Solving the equations of motion [Eqs. (23) and (24)] numerically, we obtain the trajectories in phase space presented in Fig. 1. From this figure, we can see the existence of three disjoint regions related with the sign of λ:

(1) $\lambda > 0$: Region colored in light blue, corresponding to the triangle $x_1 + x_2 < 1$. This is where the stable fixed point *I* is located, therefore leading all trajectories inside this region toward a universe in eternal inflation.
(2) $\lambda = 0$: Region in light brown, corresponding to the line $x_1 + x_2 = 1$ and a CDM universe. In this region, the trajectories flow from the unstable fixed point *III*, corresponding to a radiation-dominated epoch, towards the saddle fixed point *II*, corresponding to a matter-dominated epoch.
(3) $\lambda < 0$: Region in dark blue, corresponding to the plane $x_1 + x_2 > 1$. It has no fixed points, and all trajectories diverge towards infinity, with *E* asymptotically approaching zero.

In order to agree with the observations of an expanding Universe, the value of λ must be positive. This is what was obtained in Ref. [27], where this model was constrained using SnIa, baryonic acoustic oscillations, cosmic chronometers, and redshift space distortions.

Qualitatively, the previous dynamical system is similar to a ΛCDM universe where the value of the cosmological constant can be positive, negative, or zero [29]. However, in ΛCDM with a negative cosmological constant, the universe eventually collapses into a big crunch.

C. Computing the value of λ

In order to compute the value of λ, we evaluate Eq. (16) at the present day, obtaining

$$\left(\lambda - \frac{1}{2}\right) e^{\lambda - 1/2} = -\frac{\Omega_m + \Omega_r}{2\sqrt{e}}. \tag{28}$$

This equation only possesses a solution provided that $\Omega_m + \Omega_r \leq 2e^{-1/2}$. This is not immediately ensured, because the sum of the densities is not necessarily equal to 1. The two possible solutions for λ are

$$\lambda_0 = \frac{1}{2} + W_0\left(-\frac{\Omega_m + \Omega_r}{2e^{1/2}}\right), \tag{29}$$

$$\lambda_{-1} = \frac{1}{2} + W_{-1}\left(-\frac{\Omega_m + \Omega_r}{2e^{1/2}}\right), \tag{30}$$

where W_0 and W_{-1} are the main and the -1 branches of the Lambert function, respectively.

We discard the solution λ_{-1}, since it only provides negative values for λ. Additionally, we see that λ_0 takes negative values when $\Omega_m + \Omega_r > 1$; hence, for λ to be positive, the sum of these densities must be smaller than or equal to 1 as in ΛCDM.

IV. DATASETS

Throughout this work, we make use of two different sources of observational data, SnIa and CMB, and of mock catalogs for SS events generated for the LISA space mission and ET.

A. Type-Ia supernovae

We use SnIa to provide low-redshift constraints for this model. The dataset of SnIa used is the Pantheon sample [30], with the corresponding data publicly available in [31]. For performance reasons, the binned sample of this dataset was used.

The relationship between the apparent magnitude and the luminosity distance is given by

$$m = M + 5\log\left(\frac{d_L(z)}{\text{Mpc}}\right) + 25, \tag{31}$$

where *M* is the bolometric magnitude. In order to avoid degeneracies and unwanted parameters, we followed the procedure presented in [32], where a marginalization was

performed on both H_0 and the bolometric magnitude. The likelihood for the SnIa reads

$$L = \exp\left[-\frac{1}{2}\left(A - \frac{B^2}{C}\right)\right], \tag{32}$$

where A, B, and C are defined as

$$A = \sum_{i=1}^{n} \frac{\Delta^2(z_i)}{\sigma^2(z_i)}, \qquad B = \sum_{i=1}^{n} \frac{\Delta(z_i)}{\sigma^2(z_i)}, \qquad C = \sum_{i=1}^{n} \frac{1}{\sigma^2(z_i)}, \tag{33}$$

with $\sigma(z)$ representing the error for each SnIa measurement at redshift z_i, and where

$$\Delta(z_i) = m^{(\mathrm{obs})}(z_i) - 5\log\left(\frac{H_0}{c} d_L(z_i)\right) \tag{34}$$

is the difference between the observed magnitude $m^{(\mathrm{obs})}$ and the H_0-independent luminosity distance.

B. Cosmic microwave background radiation

In order to assess the behavior of this model at high redshifts, we condense the information provided by the CMB into what are known as the shift parameters [33]:

$$R = \sqrt{\Omega_b + \Omega_c}\frac{H_0}{c} r(z_*), \tag{35}$$

$$l_a = \pi \frac{r(z_*)}{r_s(z_*)}, \tag{36}$$

$$\omega_b = \Omega_b h^2, \tag{37}$$

where $\Omega_m = \Omega_b + \Omega_c$ is the sum of the baryonic and dark matter densities, $r(z)$ is the comoving distance

$$r(z) = \int_0^z \frac{c}{H(z)} dz, \tag{38}$$

and $r_s(z)$ is the comoving sound horizon

$$r_s(z) = \int_z^\infty \frac{c_s(z)}{H(z)} dz, \tag{39}$$

with $c_s(z)$ being the sound speed as a function of redshift:

$$c_s(z) = \frac{c}{\sqrt{3(1 + \hat{R}_b/(1+z))}}, \tag{40}$$

where $\hat{R}_b$ is given by

$$\hat{R}_b = 31,500 \Omega_b h^2 \left(\frac{T_{\mathrm{CMB}}}{2.7\ \mathrm{K}}\right)^{-4}, \tag{41}$$

with the temperature of the CMB being taken as $T_{\mathrm{CMB}} = 2.7255$ K.

We can compute the value of the redshift of photon decoupling surface, z_*, as [34]

$$z_* = 1048\left[1 + \frac{0.00124}{(\Omega_b h^2)^{0.738}}\right][1 + g_1(\Omega_m h^2)^{g_2}], \tag{42}$$

where g_1 and g_2 are

$$g_1 = \frac{0.0783(\Omega_b h^2)^{-0.238}}{1 + 39.5(\Omega_b h^2)^{-0.763}}, \tag{43}$$

$$g_2 = 0.560[1 + 21.1(\Omega_b h^2)^{1.81}]^{-1}. \tag{44}$$

Besides the shift parameters, we fix the value of $\omega_r = \Omega_r h^2$ to $\omega_r = 4.15 \times 10^{-5}$.

We consider a Gaussian likelihood of the form

$$L = \exp\left(-\frac{1}{2}\vec{x}^T C^{-1} \vec{x}\right), \tag{45}$$

where $\vec{x} = (l_a - l_a^{(\mathrm{exp})}, R - R^{(\mathrm{exp})}, \omega_b - \omega_b^{(\mathrm{exp})})$ is the vector formed by the theoretical prediction and the measurements of the three quantities defined above. C^{-1} is the inverse of the covariance matrix. Both the observational values and the covariance matrix were taken from the Planck 2018 TT + lowE release [35,36].

C. Standard sirens

Even though this model of $f(Q)$ quickly recovers GR as the redshift increases, the GW luminosity distance, presented previously in Eq. (19), is not identical to the standard luminosity distance function. Due to the lack of constraining power coming from current SS events, we instead rely on forecast data in order to assess the potential that current and future GW observatories will have in constraining this model.

To generate the mock catalogs of SS events, we took the procedure presented in [37], where mock catalogs for the Laser Interferometer Gravitational-Wave Observatory (LIGO), LISA, and the ET were developed. In short, the authors took the theoretical expected distribution of observed SS events and the expected error for each measurement for a given observatory, and, assuming a ΛCDM cosmological model in agreement with SnIa, generated catalogs of SS events consisting of a redshift z, the value of the luminosity distance $d_{\mathrm{GW}}(z)$, and its corresponding error $\sigma(z)$.

For this analysis, we considered two distinct cases: an ET catalog, with 1000 events, and a LISA catalog, with 15

events and a constraining power corresponding to the median of the generated catalogs in the previously mentioned article. We considered mock catalogs for LIGO but did not use them here, as the events provided do not place substantial constraints.

We consider a standard Gaussian likelihood for this dataset of the form

$$L = \exp\left(-\frac{1}{2}\sum_{i=0}^{N}\left[\frac{d_{\mathrm{GW}}^{(\mathrm{obs})}(z_i) - d_{\mathrm{GW}}(z_i)}{\sigma(z_i)}\right]^2\right), \quad (46)$$

where $\sigma(z_i)$ represents the error of the measurement of the SS events with redshift z_i with the corresponding observed luminosity distance $d_{\mathrm{GW}}^{(\mathrm{obs})}(z_i)$, and N represents the number of SS events in each catalog.

V. CONSTRAINTS

A. Bayesian inference methodology

We performed a Bayesian analysis using Markov chain Monte Carlo (MCMC) methods. We use PyStan [38], a Python interface to Stan [39], a statistical programming language that implements the No-U-turn sampler, a variant of the Hamiltonian Monte Carlo. The output was then analyzed using the GetDist [40] and ArviZ [41] Python packages that allow for an exploratory analysis of Bayesian models.

For each run, we executed at least four independent chains, each with at least 2500 samples on the posterior distribution and at least 2500 warm-up steps. To ensure that the chains converged, we used the $\hat{R}$ diagnostic, a convergence test introduced in [42]. This diagnostic indicates how well the different chains are mixed together and whether they have converged. We have only used samples that have $\hat{R} \leq 1.05$, where $\hat{R} = 1$ represents perfect convergence.

The initial values are randomly sampled from a Gaussian distribution with a mean around the expected value and a standard deviation of order 10% of the corresponding mean for each parameter.

We considered weakly informative priors on each parameter, specifically a Gaussian distribution centered on the expected value with a standard deviation 2 orders of magnitude larger. This ensures a quasiflat prior around the region of interest.

B. Results and discussion

Using the methodology described in the previous subsection, we used the datasets presented in Sec. IV to constrain both the $f(Q)$ model under study and ΛCDM.

Starting with the constraints on ΛCDM, the corner plot is presented in Fig. 2, and the best-fit values with the corresponding 1σ region are presented in Table II.

From Fig. 2, we can see that in ΛCDM there is an agreement in the value of Ω_m for all datasets, with LISA showing higher error bars when compared to the other datasets. As for the value of h, there is a slight disagreement between the CMB and the SS mock catalogs, given that the mock catalogs used, constructed in [37], had $h = 0.7$ as the fiducial value.

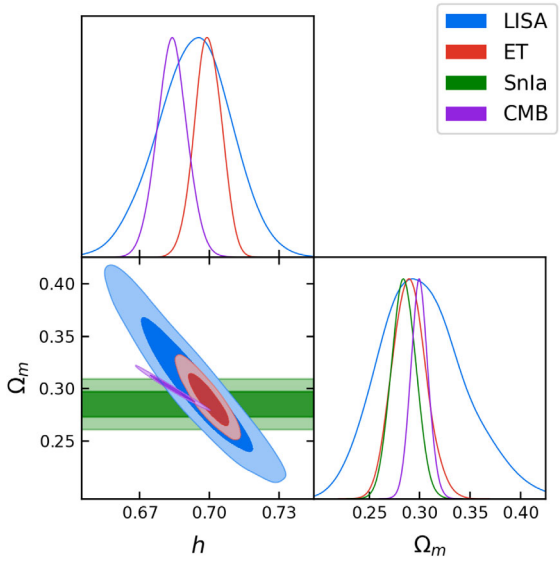

FIG. 2. Constraints set by SnIa, CMB shift parameters, and forecast SS events for the ET, and a median LISA catalog for ΛCDM.

For the $f(Q)$ model, the corner plot is presented in Fig. 3, and the best-fit values, with the corresponding 1σ region, are presented in Table III. We can immediately see that there are tensions in both Ω_m and h in this model.

The best-fit value we obtained for Ω_m using SnIa is consistent with the analysis made in [27] that also includes baryonic acoustic oscillations and cosmic chronometers. The value $\Omega_m \simeq 0.335$ differs from the one obtained for ΛCDM, $\Omega_m \simeq 0.285$—not surprisingly, given that the low redshift [Eq. (18)] includes a multiplicative factor $e^{-\lambda}$.

On the other hand, the SnIa value for Ω_m is in tension with the value we obtain using CMB. This happens because the CMB takes into account a cumulative effect from high to low redshifts, thus considering both limits [Eqs. (17) and (18)].

We observe that the Ω_m values of SnIa and SS are also in tension. It is true that both observables probe the same low-redshift regime; however, their luminosity distances are different due to the modified gravity factor seen in Eq. (19). This extra factor fully explains the tension between the two

TABLE II. Best fit and 1σ error set by SnIa, CMB, and forecast SS events for LISA and the ET, for ΛCDM.

	SnIa	CMB	LISA	ET
Ω_m	0.285 ± 0.012	0.300 ± 0.009	$0.304^{+0.035}_{-0.048}$	0.290 ± 0.017
h	⋯	0.684 ± 0.007	0.694 ± 0.016	0.699 ± 0.006

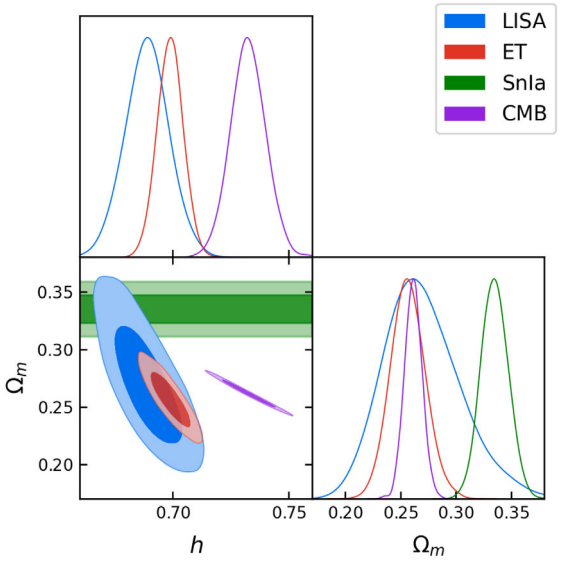

FIG. 3. Constraints set by SnIa, CMB shift parameters, and forecast SS events for the ET and the median case for LISA, for the model of $f(Q)$ presented in Eq. (15).

TABLE III. Best fit and 1σ error set by SnIa, CMB, and forecast SS events for LISA and the ET, for the model of $f(Q)$ under study.

	SnIa	CMB	LISA	ET
Ω_m	0.335 ± 0.012	0.262 ± 0.008	$0.270^{+0.029}_{-0.039}$	0.257 ± 0.016
h	⋯	0.732 ± 0.008	0.689 ± 0.009	0.699 ± 0.006

measurements and can be seen as a direct test of the existence of a modified gravity term. We have verified that the tension in Ω_m between the SS events and SnIa disappears, removing this correction from the luminosity distance of GWs. This analysis shows that comparing future SS events with standard candles can be decisive in testing modified gravity models using low-redshift observables alone.

As in the case of the SnIa and CMB, we also expect to see a tension arising between the GW observables and the CMB. This tension, however, depends on the specific choices for the fiducial values used in the SS mock data. In this instance, we can see a clear tension between the measurements of h, but comparable values for Ω_m. This latter result is just a coincidence occurring for this particular choice of h, and is unlikely to be a general feature.

VI. CONCLUSIONS

We studied an $f(Q)$ modification of gravity that accounts for the late-time accelerated expansion of the Universe without adding a cosmological constant. This modification has the same number of free parameters as the standard ΛCDM model; albeit, the propagation of tensorial perturbations introduces a change in the luminosity distance of GWs.

We used a dynamical system analysis to reveal the existence of three fixed points and three disjoint regions in the phase space defined by the sign of the parameter λ. For $\lambda < 0$, we identified a region characterized by trajectories where $E(z) \to 0$ as the scale factor increases. When $\lambda = 0$, we recover a CDM universe with a radiation followed by a matter epoch. When $\lambda > 0$, the stable fixed point corresponds to a regime of eternal inflation, meaning that this case can lead to a viable universe with a late-time accelerated expansion without an explicit cosmological constant.

First, we constrained this model using SnIa, recovering the value of Ω_m obtained previously in [27], where other low-redshift observations were also used. This value is, not surprisingly, different from the best fit found for a ΛCDM, given the factor $e^{-\lambda}\Omega_m$ in the modified Friedmann equation (18).

We made an independent constraint using high-redshift measurements from CMB and verified that the best-fit value for Ω_m is in tension with the value obtained with SnIa. We conclude that this is a manifestation of differing high- and low-redshift limits of the model, which CMB takes into account but SnIa does not. In order to keep the attractive features of this model at low redshifts, the form of $f(Q)$ needs to be somehow modified at high redshifts to make it consistent with CMB data.

As is, the current data disfavor this model already at the background level. This is a common feature in models of modified gravity that depart from ΛCDM. $f(T)$ and $f(Q)$ models can be shown to be equivalent in FLRW, whereas $f(R)$ models, though being formally distinguishable, must in practice have a similar cosmological evolution. In particular, $f(R)$ models have their free parameters strongly constrained to be very close to the ΛCDM limit [43], which seems also to be the case for $f(T)$ and $f(Q)$ [16,44,45].

Finally, we used mock catalogs of SS constructed with ΛCDM as the fiducial model. As expected, the modified luminosity distance for gravitational waves raises a tension with the SnIa results, implying that in the future, this feature will immediately discriminate this model from ΛCDM.

Although current data (CMB and SnIa) already disfavor this model, this study provides a working example of how future SS events, measured both by LISA and the ET, will play a fundamental role when testing models of modified gravity using low-redshift data alone.

ACKNOWLEDGMENTS

The authors are thankful to Fotis Anagnostopoulos for the fruitful discussions. The authors acknowledge support from Fundação para a Ciência e a Tecnologia via the following projects: No. UIDB/04434/2020 & No. UIDP/04434/2020, No. CERN/FIS-PAR/0037/2019, No. PTDC/FIS-OUT/29048/2017, COMPETE2020: No. POCI-01-0145-FEDER-028987 & FCT: No. PTDC/FIS-AST/28987/2017, No. PTDC/FIS-AST/0054/2021, No. EXPL/FIS-AST/1368/2021.

[1] L. Perivolaropoulos and F. Skara, Challenges for ΛCDM: An update, New Astron. Rev. **95**, 101659 (2022).
[2] J. B. Jiménez, L. Heisenberg, and T. Koivisto, The geometrical trinity of gravity, Universe **5**, 173 (2019).
[3] J. B. Jimenez, L. Heisenberg, and T. Koivisto, Coincident general relativity, Phys. Rev. D **98**, 044048 (2018).
[4] R.-G. Cai and T. Yang, Estimating cosmological parameters by the simulated data of gravitational waves from the Einstein Telescope, Phys. Rev. D **95**, 044024 (2017).
[5] *Modified Gravity and Cosmology*, edited by E. N. Saridakis, R. Lazkoz, V. Salzano, P. V. Moniz, S. Capozziello, J. B. Jiménez, M. D. Laurentis, and G. J. Olmo (Springer International Publishing, New York, 2021).
[6] I. Ayuso, R. Lazkoz, and J. P. Mimoso, DGP and DGP-like cosmologies from $f(Q)$ actions, Phys. Rev. D **105**, 083534 (2022).
[7] B. J. Barros, T. Barreiro, T. Koivisto, and N. J. Nunes, Testing $F(Q)$ gravity with redshift space distortions, Phys. Dark Universe **30**, 100616 (2020).
[8] E. Belgacem, Y. Dirian, S. Foffa, and M. Maggiore, The gravitational-wave luminosity distance in modified gravity theories, Phys. Rev. D **97**, 104066 (2018).
[9] I. S. Albuquerque and N. Frusciante, A designer approach to $f(Q)$ gravity and cosmological implications, Phys. Dark Universe **35**, 100980 (2022).
[10] L. Atayde and N. Frusciante, $f(Q)$ gravity and neutrino physics, Phys. Rev. D **107**, 124048 (2023).
[11] L. Atayde and N. Frusciante, Can $f(Q)$ gravity challenge ΛCDM?, Phys. Rev. D **104**, 064052 (2021).
[12] N. Frusciante, Signatures of $f(Q)$ gravity in cosmology, Phys. Rev. D **103**, 044021 (2021).
[13] S. Capozziello, V. D. Falco, and C. Ferrara, Comparing equivalent gravities: Common features and differences, Eur. Phys. J. C **82**, 865 (2022).
[14] C. Krishnan, E. Ó. Colgáin, M. Sheikh-Jabbari, and T. Yang, Running Hubble tension and a h_0 diagnostic, Phys. Rev. D **103**, 103509 (2021).
[15] W. Khyllep, A. Paliathanasis, and J. Dutta, Cosmological solutions and growth index of matter perturbations in $f(Q)$ gravity, Phys. Rev. D **103**, 103521 (2021).
[16] I. Ayuso, R. Lazkoz, and V. Salzano, Observational constraints on cosmological solutions of $f(Q)$ theories, Phys. Rev. D **103**, 063505 (2021).
[17] B. P. Abbott *et al.* (LIGO Scientific and Virgo Collaborations), GW170817: Observation of Gravitational Waves from a Binary Neutron Star Inspiral, Phys. Rev. Lett. **119**, 161101 (2017).
[18] LIGO Scientific and Virgo Collaborations, Properties and astrophysical implications of the $150M_\odot$ binary black hole merger GW190521, Astrophys. J. Lett. **900**, L13 (2020).
[19] M. J. Graham *et al.*, Candidate Electromagnetic Counterpart to the Binary Black Hole Merger Gravitational Wave Event S190521g, Phys. Rev. Lett. **124**, 251102 (2020).
[20] P. Amaro-Seoane *et al.*, Laser interferometer space antenna, arXiv:1702.00786.
[21] P. Auclair *et al.* (The LISA Cosmology Working Group), Cosmology with the laser interferometer space antenna, Living Rev. Relativity **26**, 5 (2023).
[22] https://github.com/jpmvferreira/testing-L-free-fQ-cosmology.
[23] L. Järv, M. Rünkla, M. Saal, and O. Vilson, Nonmetricity formulation of general relativity and its scalar-tensor extension, Phys. Rev. D **97**, 124025 (2018).
[24] J. B. Jiménez, L. Heisenberg, T. S. Koivisto, and S. Pekar, Cosmology in $f(Q)$ geometry, Phys. Rev. D **101**, 103507 (2020).
[25] J. Jiménez, L. Heisenberg, and T. S. Koivisto, Teleparallel Palatini theories, J. Cosmol. Astropart. Phys. 08 (2018) 039.
[26] T. Koivisto, A note on covariant conservation of energy-momentum in modified gravities, Classical Quantum Gravity **23**, 4289 (2006).
[27] F. K. Anagnostopoulos, S. Basilakos, and E. N. Saridakis, First evidence that non-metricity $f(Q)$ gravity could challenge ΛCDM, Phys. Lett. B **822**, 136634 (2021).
[28] F. K. Anagnostopoulos, V. Gakis, E. N. Saridakis, and S. Basilakos, New models and big bang nucleosynthesis constraints in $f(Q)$ gravity, Eur. Phys. J. C **83**, 58 (2023).
[29] S. Bahamonde, C. G. Böhmer, S. Carloni, E. J. Copeland, W. Fang, and N. Tamanini, Dynamical systems applied to cosmology: Dark energy and modified gravity, Phys. Rep. **775–777**, 1 (2018).
[30] D. M. Scolnic *et al.* (Pan-STARRS1 Collaboration), The complete light-curve sample of spectroscopically confirmed type Ia supernovae from Pan-STARRS1 and cosmological constraints from the combined Pantheon sample, Astrophys. J. **859**, 101 (2018).
[31] https://github.com/dscolnic/Pantheon.
[32] M. Goliath, R. Amanullah, P. Astier, A. Goobar, and R. Pain, Supernovae and the nature of the dark energy, Astron. Astrophys. **380**, 6 (2001).
[33] Z. Zhai and Y. Wang, Robust and model-independent cosmological constraints from distance measurements, J. Cosmol. Astropart. Phys. 07 (2019) 005.
[34] W. Hu and N. Sugiyama, Small-scale cosmological perturbations: An analytic approach, Astrophys. J. **471**, 542 (1996).
[35] J. d. C. Perez, J. S. Peracaula, and C. P. Singh, Running vacuum in Brans-Dicke theory: A possible cure for the σ_8 and H_0 tensions, arXiv:2302.04807.
[36] P. Collaboration, Planck 2018 results, Astron. Astrophys. **641**, A6 (2020).
[37] J. Ferreira, T. Barreiro, J. Mimoso, and N. J. Nunes, Forecasting $F(Q)$ cosmology with ΛCDM background using standard sirens, Phys. Rev. D **105**, 123531 (2022).
[38] A. Riddell, A. Hartikainen, and M. Carter, PyStan (3.0.0), PyPi (2021).
[39] S. D. Team, *Stan Modeling Language Users Guide and Reference Manual* (2021), 2nd ed.
[40] A. Lewis, GetDist: A Python package for analysing Monte Carlo samples, arXiv:1910.13970.
[41] R. Kumar, C. Carroll, A. Hartikainen, and O. Martin, ArviZ a unified library for exploratory analysis of Bayesian models in Python, J. Open Source Software **4**, 1143 (2019).

[42] A. Vehtari, A. Gelman, D. Simpson, B. Carpenter, and P.-C. Bürkner, Rank-normalization, folding, and localization: An improved $\widehat{R}$ for assessing convergence of MCMC (with discussion), Bayesian Anal. **16**, 667 (2021).

[43] R. C. Nunes, S. Pan, E. N. Saridakis, and E. M. Abreu, New observational constraints on $f(R)$ gravity from cosmic chronometers, J. Cosmol. Astropart. Phys. 01 (2017) 005.

[44] F. B. M. dos Santos, J. E. Gonzalez, and R. Silva, Observational constraints on $f(T)$ gravity from model-independent data, Eur. Phys. J. C **82**, 823 (2022).

[45] R. Lazkoz, F. S. N. Lobo, M. Ortiz-Baños, and V. Salzano, Observational constraints of $f(Q)$ gravity, Phys. Rev. D **100**, 104027 (2019).